van der Waals atomic trap in a scanning-tunneling-microscope junction:
Tip shape, dynamical effects, and tunnel current signatures

X. Bouju* and Ch. Girard

Laboratoire de Physique Moléculaire, UMR CNRS 6624, Université de Franche-Comté, F-25030 Besançon Cedex, France

H. Tang, C. Joachim, and L. Pizzagalli[†]

Centre d'Élaboration de Matériaux et d'Études Structurales, UPR CNRS 8011, 29 rue Jeanne-Marvig, Boîte Postale 4347, F-31055 Toulouse Cedex 4, France

The growing interest in the study of artificial nanoscale structures stabilized by a corrugated surface calls for specific models adapted to the low symmetry of such systems. In the case of physisorbed species, such atomic patterns can be realized by controlling the magnitude of the van der Waals trap generated by the apex of a thin metal tip. In this work, the van der Waals interaction between a Cu(110) surface, a xenon atom, and the copper probe tip of a scanning tunneling microscope (STM) is investigated. The dispersion energy contribution between the xenon atom and the discrete tip apex is determined at the N-body order by solving Dyson's equation. From this procedure, we investigate the stability of the adsorbate for different shapes and sizes of the probe. When we consider the entire STM junction, a van der Waals trap occurs within a small tip-surface spacing. The magnitude of this trap can reach about 30 meV, which has to be compared with the physisorption energy of ~ 180 meV of a single xenon atom on the Cu(110) surface. From this model system the important question of the atomic displacement with a STM tip, as realized experimentally by Eigler and Schweizer [Nature **344**, 524 (1990)], is revisited. To achieve this purpose, we have studied the dynamical atomic dragging with the [100], [110], and [111] oriented tips: We have found that the adsorbate is pulled by the [110] tip and is displaced in front of the two other types of tip. Finally, by calculating the tunnel current during the motion of the adsorbate in the junction, we were able to extract a *current signature* directly related to the nature of the moving process. [S0163-1829(97)02824-5]

I. INTRODUCTION

The van der Waals (vdW) interactions have been widely studied for some seventy years. In the context of surface science, the precise determination of this fundamental quantity, which is responsible for the stabilization of adsorbed species (atoms or molecules) on many surfaces, has generated a lot of theoretical analysis.[1–3] Only very recently these pioneering approaches have been revisited within the framework of the density-functional theory.[4,5]

In the context of scanning probe techniques, the precise computation of the vdW energy part is mandatory when dealing with physisorbed species. The first consequence of these interactions is to modify the image-object relation, not only with a scanning tunneling microscope (STM) but also with an atomic force microscope. On the other hand, such probe-adsorbate interactions can be turned into an advantage by using them to reposition one by one atoms or molecules in a controlled manner.[6] The first experiment was realized by Eigler and Schweizer.[7] They succeeded in manipulating individual xenon atoms with the tip of a STM and creating artificial atomic structures stabilized on a metallic surface. To explain this manipulation process, they proposed a physical mechanism in which attractive forces between the tip and the adsorbate are involved: the xenon atom is thus slid on the corrugated surface. Since this pioneering work, several nanostructures have been fabricated on surfaces with a local probe. Crommie *et al.*[8,9] have built a ''quantum corral'' with iron atoms on Cu(111) surface, Zeppenfeld *et al.*[10] have built

''CO man'' with carbon oxide molecules on Pt(111), and Meyer *et al.*[11] have performed similar experiments on the CO/Cu(221) system. More recently, a series of room-temperature experiments has been realized with different systems, including Cu-TBP-porphyrin molecules on a copper surface[12] and C_{60} molecules on metallic substrates.[13–15]

To describe such experiments qualitatively, it is necessary to calculate accurately the interactions between all the atoms constituting the STM junction. In a previous work,[16] we have evaluated the adsorption energy of a xenon atom near a STM tip taking into account the two- and three-body dipolar terms. Then we studied[17] the sliding process of a Xe atom on the Cu(110) surface with a STM Cu[110] oriented tip. A static study of the potential surface permitted us to determine the tip-sample distance threshold for the atomic manipulation. Since then, several theoretical studies have described the Xe atom repositioning by a local probe tip based on two-body interaction vdW potentials.[17–23]

In the present paper, we propose from the same model system the description of the vdW energy calculation following a self-consistent scheme able to include the entire N-body interaction series. In a second step, we address the question of the differential tip effect on the adsorption state under the STM tip and the magnitude of the resulting vdW trap in the junction. In Sec. IV, from a dynamical study of the motion of the atom we provide useful hints about the repositioning mecanisms for both different tip shapes and tip-surface distances. Finally, we analyze the variation of the tunneling current intensity in the STM junction during the
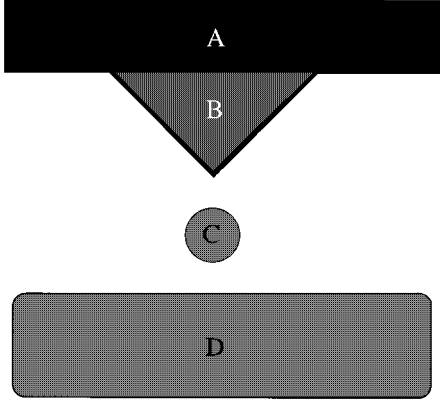
FIG. 1. Schematic model of the system considered: the tip body (A), the tip apex (B), the adsorbate (C), and the substrate (D).

manipulation of a Xe atom by the local probe tip. It is then demonstrated that each manipulation mode has a specific and easily identifiable signature in the tunneling current.

II. DESCRIPTION OF THE INTERACTIONS

A. Model and theoretical background

The STM junction considered here consists of four distinct parts (Fig. 1): the tip body (A), the tip apex (B), the adsorbate (C), and the substrate (D). Both the substrate and tip body are made of copper. In the numerical work to be discussed in this paper, the tip body can support three different apexes with [111], [110], or [100] structures, and the adsorbate is a xenon atom. The substrate is cleaved to present a Cu(110) face. Notice that a nickel surface was used in the experiment of Eigler and Schweizer.[7] Nevertheless, the choice of a copper substrate will not modify the physical understanding of the manipulation process, and the Xe adsorption is well known on Cu(110) with no ambiguities about its physisorption sites. In order to determine the behavior of the Xe atom in this junction, we have calculated its potential energy U_C, which can be separated into three terms

$$U_C(\mathbf{r}) = U_{CD}(\mathbf{r}) + U_{CA}(\mathbf{r}) + U_{CB}(\mathbf{r}), \qquad (1)$$

with $\mathbf{r} = (x, y, z)$ the Xe atom coordinates. The first term on the right-hand side of Eq. (1) describes the interaction between the adsorbate and the surface. A Born-Mayer-like potential was chosen with a dipolar and a quadrupolar contribution

$$U_{CD}(\mathbf{r}) = \sum_i \left(-\frac{C_6}{|\mathbf{r} - \mathbf{r}_i|^6} - \frac{C_8}{|\mathbf{r} - \mathbf{r}_i|^8} + A_0 e^{-\sigma|\mathbf{r} - \mathbf{r}_i|} \right), \quad (2)$$

where $\{\mathbf{r}_i\}$ are the coordinates of the substrate atoms. The summation runs over the atoms constituting a Cu(110) surface, i.e., a slab with 10 planes and 169 atoms per plane. The C_6 and C_8 coefficients can be expressed with the dipolar and quadrupolar vdW parameters C_3 and C_5 available in the literature for the couple Xe-Cu:[24,25] $C_6 = 6 d \mathcal{A} C_3 / \pi$ and $C_8 = 15 d \mathcal{A} C_5 / \pi$, where d represents the distance between two discretized planes and $\mathcal{A}$ the unit cell area of the surface. The parameters of the repulsive potential A_0 and σ, fitted to obtain concordance with experimental desorption heat values,[26] have been chosen to be equal to 290.4 a.u., and

TABLE I. Number of atoms constituting the tip apex for different tip structures.

Plane number	Tip structure [110] and [100]	Tip structure [111]
1	1	1
2	5	4
3	14	11
4	30	23
5	55	42
6	91	69
7	140	106

6.614 a.u., respectively.[17] Second, the term U_{CA} between the tip body is just described by attractive terms corresponding to the vdW interaction

$$U_{CA}(\mathbf{r}) = \sum_p -d \left(\frac{3 C_3}{|z - z_p|^4} + \frac{5 C_5}{|z - z_p|^6} \right), \qquad (3)$$

with d the tip body interplane distance and z_p the z coordinate of the plane number p. No repulsive contribution is taking into account in Eq. (3) because such an energy will be negligible in the range of tip body-adsorbate distances considered here. Finally, the interaction energy between the adsorbate and the discrete tip apex has the form

$$U_{CB}(\mathbf{r}) = V_{Nb}^{dip}(\mathbf{r}) + \sum_{j=1}^{n} \left(-\frac{C_8}{|\mathbf{r} - \mathbf{r}_j|^8} + A_0 e^{-\sigma|\mathbf{r} - \mathbf{r}_j|} \right). \quad (4)$$

The positions of the n tip atoms are represented by the $\{\mathbf{r}_j\}$ vectors set and V_{Nb}^{dip} is the dipolar N-body interaction term between the adsorbate and the tip apex atoms. Table I summarizes the variation of n according to the tip structure.

In the absence of all permanent electric multipoles and following the approach of van Kampen et al.,[2] the vdW interactions V_{Nb}^{dip} can be calculated by differentiating the zero-point energies of the adsorbate when it is close to and infinitely far away from the discretized tip. In other words, we have to evaluate the electromagnetic coupled modes, which are roots of a dispersion equation associated with the considered system. This calculation scheme has been applied in numerous situations. For example, several studies have been devoted to the physisorption in confined geometries, such as zeolites, or near the edge of a straight material wedge of arbitrary opening angles.[27–29] These works showed that the physisorption energy of molecules is enhanced due to surface curvature and confinement effects and also that many-body contributions can be important in particular cases.

According to the vdW energy description from the coupled-mode method,[2] the V_{Nb}^{dip} term can be expressed with the logarithm of the dispersion equation associated with the whole system,

$$V_{Nb}^{dip}(\mathbf{r}) = \frac{\hbar}{2\pi} \int_0^\infty \ln\{\det[\mathbf{I} - \mathbf{B}(\mathbf{r}, iu)]\} du. \qquad (5)$$

The N-body character of the interaction appears in the determinant calculation and therefore in the knowledge of the matrix $\mathbf{B}$. This matrix results from the tensorial contraction

$$\mathbf{B}(\mathbf{r},\omega) = \underline{\alpha}_C(\omega) \cdot \mathbf{S}_n(\mathbf{r},\mathbf{r},\omega), \qquad (6)$$

where $\underline{\alpha}_C$ is the polarizability tensor of the adsorbate and $\mathbf{S}_n$ is the dyadic tensor describing the field susceptibility of the adsorbate in the presence of the n tip apex atoms. This tensorial quantity can be accurately evaluated by introducing an iterative scheme associated with a sequence of Dyson's equations.

B. Dyson's sequence

For our problem, the integral form of Dyson's equation is

$$\mathbf{S}_n(\mathbf{r},\mathbf{r}',\omega) = \mathbf{S}_0(\mathbf{r},\mathbf{r}',\omega)$$

$$+ \int \mathbf{S}_0(\mathbf{r},\mathbf{r}'',\omega) \cdot \underline{\chi}(\mathbf{r}'',\omega) \cdot \mathbf{S}_n(\mathbf{r}'',\mathbf{r}',\omega) d\mathbf{r}'',$$

$$(7)$$

where $\mathbf{S}_n$ is the field susceptibility between the points $\mathbf{r}$ and $\mathbf{r}'$, and $\mathbf{S}_0$ is the dipolar propagator associated with the tip body (A). Expressions of this propagator $\mathbf{S}_0$ are available in the literature.[30] In Eq. (7), the integral runs over the volume of the tip apex (B) and χ describes the dynamical properties of the material system. In its integral form, Eq. (7) cannot be computerized easily. In order to overcome this difficulty, we apply a discretization procedure to account and calculate iteratively such a field susceptibility for each atom in the interaction.

Starting with one tip atom, we built the field susceptibility expression following the iterative procedure:

$$\mathbf{S}_i(\mathbf{r},\mathbf{r}',\omega) = \mathbf{S}_{i-1}(\mathbf{r},\mathbf{r}',\omega)$$

$$+ \mathbf{S}_{i-1}(\mathbf{r},\mathbf{r}_i,\omega) \cdot \underline{\alpha}_i(\omega) \cdot \mathbf{S}_i(\mathbf{r}_i,\mathbf{r}',\omega). \quad (8)$$

In this equation, $i = 1, \ldots, n$ (n tip apex atoms), $\mathbf{r}_i$ localizes the ith atom, and $\underline{\alpha}_i(\omega)$ is its dynamical dipolar polarizability. In the present work, each polarizability associated with each Cu atom is assumed to be identical and isotropic. Moreover, in this paper, we have neglected the many-body terms between the adsorbate, the tip apex atoms, and the bare tip body. In other words, we have considered only the N-body contributions occurring between the Xe atom and all the copper apex atoms. Such an iterative procedure, extensively described in our previous published works,[17,31,32] allows us to easily calculate the $\mathbf{S}_n$ propagator (or field susceptibility).

III. ADSORPTION INSIDE A STM JUNCTION: THE VAN DER WAALS TRAP

The mechanical interactions of an adsorbate and the tip apex is a crucial point in local probe techniques. What generally appears as a destructive drawback in the STM imaging process can be turned into an advantage in some cases. In fact, such interactions allow us to precisely manipulate atoms and molecules with a fine control of the tip position, especially in the vertical position where a precision of $10^{-2} - 10^{-3}$ Å can be achieved. In this section, we describe the xenon atom adsorption on a STM tip. In a first step, we consider just a perfect and a truncated tip to study the importance of the many-body contributions. The behavior of a
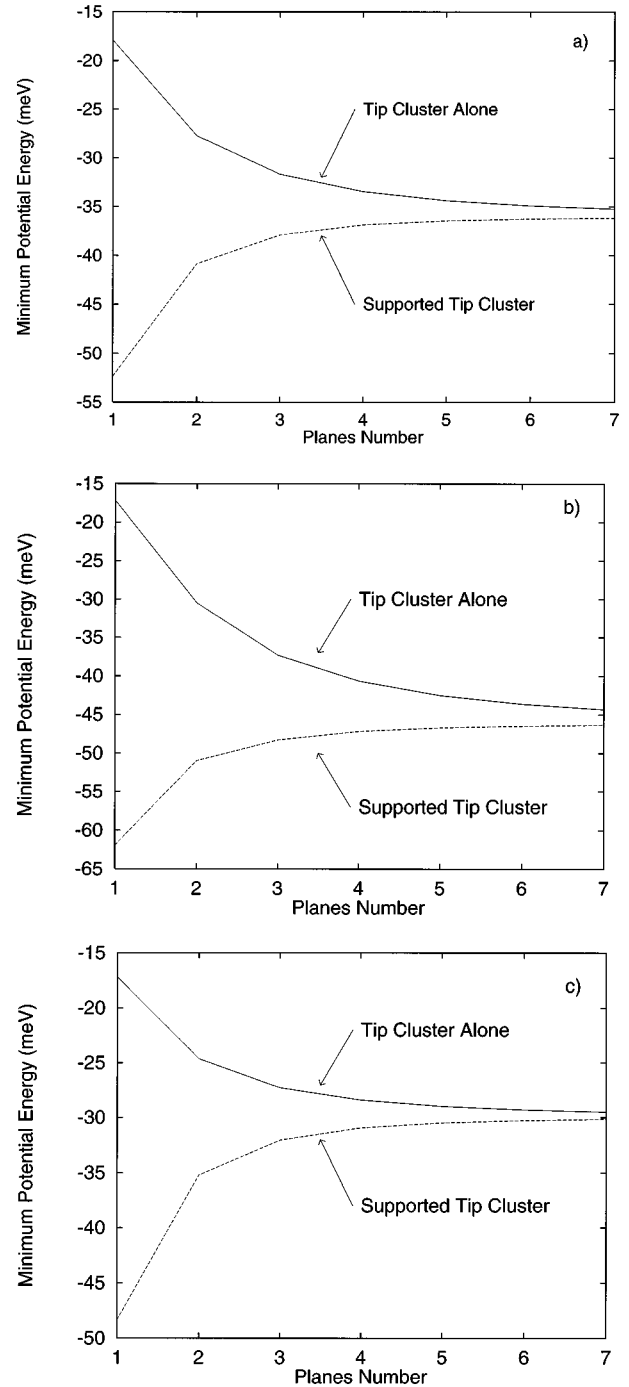

FIG. 2. Minimum adsorption energy of a Xe atom just above a copper tip versus the planes number constituting the tip apex, for a given atomic structure of a probe tip (a) [100], (b) [110], and (c) [111] oriented. In each case, the solid line represents the configuration with the tip cluster alone while the dashed line describes the adsorption comportment between the Xe atom and the cluster supported by a semi-infinite medium slab.

single xenon atom inside a full STM junction is then investigated.

A. Adsorption on a STM tip

We present the results concerning the physisorption of a xenon atom straight above a copper tip. Figures 2(a)–2(c)

TABLE II. Comparison between N-body and two-body energetic contributions in meV (N-body minus two-body terms), for a perfect and a truncated tip [110] oriented.

Plane number	Tip [110]	Tip [110] truncated
1	0.00	12.55
2	0.84	16.16
3	0.27	16.36
4	0.07	16.51
5	−0.09	16.48
6	−0.19	16.44
7	−0.26	

show the behavior of the minimum energy of the adsorbate with the three tip structures ([100], [110], and [111]) versus the size of the probe. In this study we compare the results obtained with isolated Cu clusters (part B in Fig. 1) to those obtained with supported clusters (parts A and B in Fig. 1). In Figs. 2(a)–2(c) the curves describe the evolution of the minimum energy as a function of the atomic layer number. All these curves start with a single atom ($n=1$) that represents the minimal energy interaction of the (Xe-Cu) atomic couple (-17.19 meV at 3.735 Å). We can deduce also the contribution of the continuum tip body for these systems: ~ -35, -45, and -31 meV at 3.55, 3.51, and 3.58 Å for, respectively, the [100], [110], and [111] tip body structures. This behavior was foreseeable because the more dense the surface structure supporting the tip cluster the less important the energy at the equilibrium. Moreover, the two curves on Fig. 2 tend towards the same limit (-35.7, -45.3, and -29.8 meV for, respectively, the [100], [110], and [111] tip body structures): The tip body contribution decreases when the discrete tip apex grows. The second column in Table II presents the comparison between N-body and two-body contributions. We have performed a two-body calculation by replacing the V_{Nb}^{dip} term in Eq. (4) by the summation $\sum_{j=1}^{n} -C_6/|\mathbf{r}-\mathbf{r}_j|^6$. The minimal Xe energy has been evaluated just above the tip cluster. The difference is not large because the many-body terms are not significant in this symmetrical configuration. In order to evaluate such contributions we have also considered truncated tips, namely, tips for which the copper atom ending the extremity has been removed. Such truncated STM probes have been mentioned in recent experiments[33] to be able to catch a xenon atom on the tip apex. The preceding calculations have been repeated for such tips and the results are presented in Fig. 3 and in the third column of Table II. To facilitate the discussion, the number of tip apex atoms can be identified by the number $n_{[xxx]}(p)$ where $[xxx]$ is the tip structure and p the plane number (see Table I). For example, the series $n_{[111]}(1)=1$, $n_{[111]\text{trunc}}(1)=3$, $n_{[111]}(2)=4$, and $n_{[110]}(2)=5$ allows to study the variation of the N-body contributions. The energies associated with this series are -17.19, -46.49, -24.62, and -30.46 meV, respectively [Figs. 2(c) and 3(c)]. The adsorption on the top of a truncated tip indicates clearly the importance of the many-body energy (15–20 % of the total energy). Thus, when the adsorbate is located near the facets of the tip, the many-body contributions have to be included to properly describe its energetic behavior.
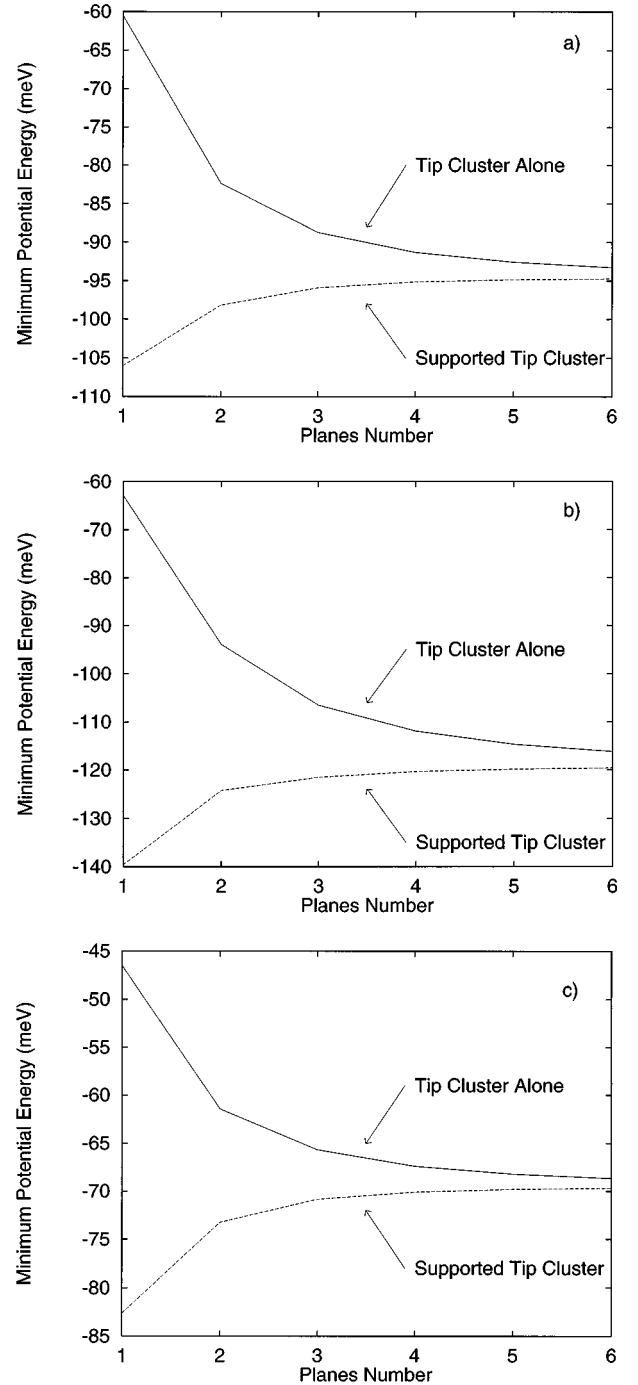

FIG. 3. Same as in Fig. 2, but for a tip configuration where the metallic atom at the extremity is missing (truncated tip).

B. A vdW trap: Cu(110)/Xe/Cu[111]

In this section, we consider a complete STM junction, i.e., the Cu(110) surface, the xenon adsorbate, and the Cu[111] probe tip. The minimal binding energy of the xenon atom on a Cu(110) surface is ~ -180 meV (dashed line in Fig. 4) and appears as a hollow site on this surface. More precisely, the minimum energy on the Cu(110) surface reveals rows along the $[\bar{1}10]$ direction (along the x axis in Fig. 5).[17] The diffusion barriers between two adjacent hollow sites are about ~ 17 meV in these channels and about ~ 32 meV perpendicular to these rows (along the [002] direction or y axis on Fig. 5).
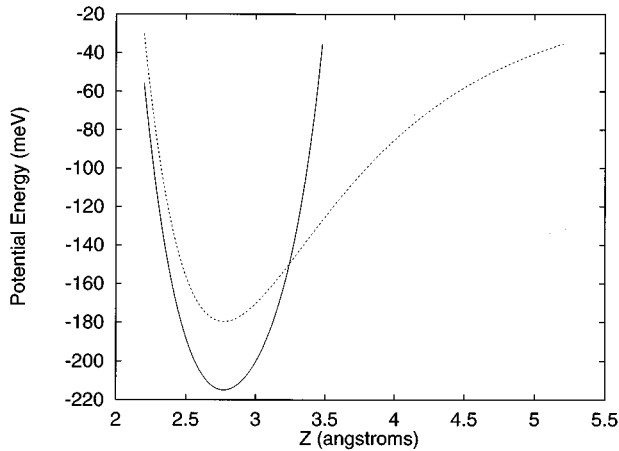
FIG. 4. Comparison between two approach curves. Dashed line, the xenon atom approaches the Cu(110) surface and the minimum adsorption energy is $U_0 = -179.71$ meV at $z_0 = 2.768$ Å from the surface; full line, the Xe atom is displaced between the surface and a copper tip [111] oriented (described by two discrete planes) placed at $z_t = 6.39$ Å. The minimum characteristics are $U_{min} = -214.91$ meV at $z_{min} = 2.770$ Å. A van der Waals trap is created by the presence of the tip with an amplitude of $U_{trap} = U_{min} - U_0 = -35.20$ meV.

When the copper tip is approached above the Cu(110) hollow site, the energy of the adsorbate is modified. Depending on the tip height, a more or less important energy trap (or meniscus) is created under the tip[17] because additional attractive or repulsive energy has been supplied by the probe. In Fig. 4 the tip is located at 6.39 Å from the surface hollow site and the adsorption energy reveals an increase of -35.20 meV, which constitutes what we called a vdW trap. The different amplitudes reached by this trap as a function of the tip size are gathered in Table III. For each probe size, we have optimized the tip-substrate distance in order to maximize the vdW trap. As expected, we recover the values of the minimum adsorption energy of the Xe atom above the copper tip alone [Fig. 2(c)]. In other words, the maximum vdW trap can be identified by the minimum energy on Figs. 2 and 3 for the tips studied in the present paper. The atoms of the probe and those of the surface are sufficiently far away to neglect vdW effects associated with the correlations between them. From Figs. 2 and 3 we remark that the vdW trap is maximum for the Cu[110] tip and minimum for the Cu[111] one. More information concerning the manipulation mecha-
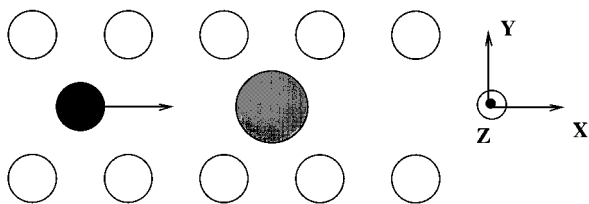

FIG. 5. Schematic geometry of the moving process: hollow circles describe the copper (110) surface atoms and the big gray one the xenon adsorbate. The last atom of the copper tip is represented by the filled black circle that is displaced along the x axis ([$\bar{1}$10] direction).

TABLE III. Minimum adsorption energy U_{min} versus the [111] tip apex size of a Xe atom placed in the probe-surface junction and the corresponding amplitude of the energetic van der Waals trap U_{trap}.

Plane number	U_{min} (meV)	U_{trap} (meV)
1	-228.06	-48.35
2	-214.91	-35.20
3	-211.75	-32.04
4	-210.65	-30.94
5	-210.20	-30.49
6	-209.98	-30.27
7	-209.87	-30.16

nisms could be extracted by exploring the entire surface potential experienced by the adsorbate. Nevertheless, to reproduce faithfully the experimental conditions, we prefer to complete our static study by a dynamical treatment.

IV. DYNAMICS OF THE Xe ATOM DRAGGING WITH A STM TIP

A. Moving processes

The dynamical problem associated with the displacement of a xenon atom under the constraint of a STM tip, scanning the sample at constant altitude, is considered in this section. In first approximation, the time-dependent positions of the adsorbate under a tip apex can be calculated in the framework of classical mechanics and thus verify Newton's equation

$$m\ddot{\mathbf{r}}(t) = -\underline{\nabla} U_C(\mathbf{r}) - \eta \dot{\mathbf{r}}(t), \qquad (9)$$

where m is the mass of the xenon atom and U_C its potential energy [see Eq. (1)]. In Eq. (9), η is a semiclassical friction coefficient accounting for the energy damping introduced by surface phonons.[34] Equation (9) is solved by a standard Verlet algorithm. In the present study the Cu(110) surface is composed of 1690 atoms, the STM probe of 3 discrete planes for the tip apex and 20 infinite planes for the tip body. A top view of the system is given in Fig. 5.

From this model system, we can distinguish three kinds of manipulation processes depending on the Xe atom position: a ''pulling'' mode, where the adsorbate remains behind the tip and is attracted by the probe; a ''sliding'' mode, in which the adsorbate is placed just under the tip and follows the probe displacement; and the ''pushing'' mode, where the adsorbate is located in front of the tip. According to the experimental results,[7] it was proposed that the xenon atom is slid along the [$\bar{1}$10] direction of the Cu(110) face, i.e., along the rows where the diffusion barriers are reduced (see Sec. III B).

Now let us examine in detail the influence of both the tip distance z_t and the tip structure at the level of the manipulation process. First, we begin with Fig. 6(a), in which we have represented a typical trajectory of the xenon atom obtained when z_t is slightly higher ($\Delta z_t = 0.05$ Å) than the tip-sample distance threshold. The potential energy calculated with the N-body contributions is presented in Fig. 6(b). This calculation has been performed with a tetragonal [110] tip contain-
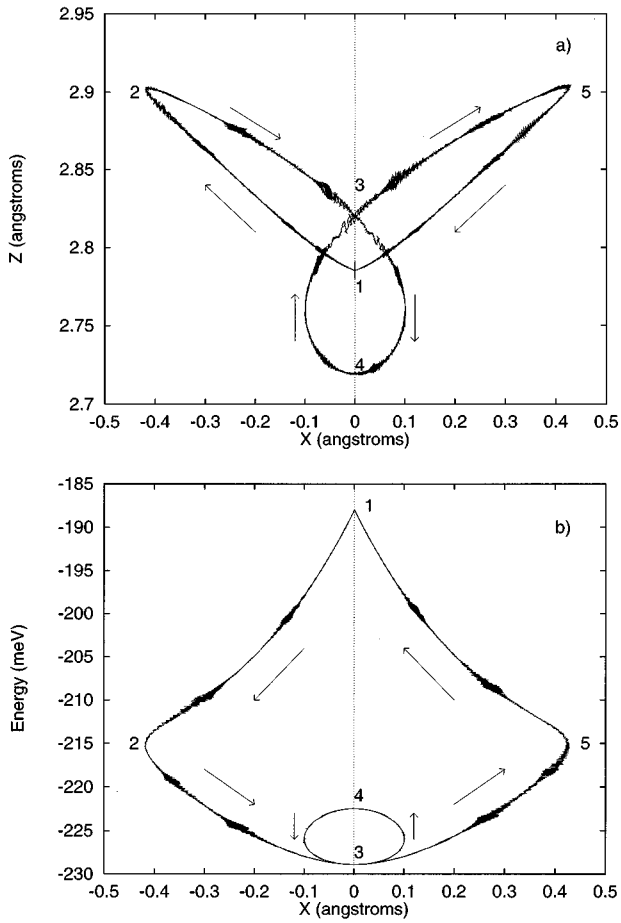
FIG. 6. Lateral displacement versus (a) vertical position z and (b) potential energy of the xenon atom during the lateral approach of a [110] oriented tip located at $z_t = 6.15$ Å. The labeled number series refers to particular points of the tip motion (see the text).

ing three discrete planes. The labeled numbers series in Fig. 6 describes different particular positions of the xenon atom versus the tip positions.

Position 1. The calculation starts when the tip apex is far enough ($x_t = -6$ Å) to leave the Xe atom in its equilibrium position ($x = y = 0$, $z = 2.78$ Å) on the surface. In this initial configuration, the semi-infinite tip body brings ~ -10 meV to the adsorbate. The tip is then approached gradually by a step of $\Delta x_t = 0.01$ Å every 100 time units (time unit = 10^{-13} s), i.e., the xenon atom is free to relax during this period. The tip velocity is several orders of magnitude faster than in real experiments, where the tip is scanned at a few angstroms per second. But what is important here is the ratio between the Xe atom relaxation time and the time interval between two tip positions. If it is small enough, the dynamics in Eq. (9) will reproduce the experiment well.

Position 2. The adsorbate is attracted by the tip apex ($x_t \sim -3$ Å) but cannot get over the diffusion barrier in the row. In other words, the tip apex does not deform the lateral barrier in the $[\bar{1}10]$ surface row enough to allow the xenon atom to pass in the preceding hollow site or above the tip.

Position 3. The tip pushes the Xe atom slightly while maintaining an attraction with it. The vdW trap increases and becomes maximum when the tip is at $x_t = -1.32$ Å. The
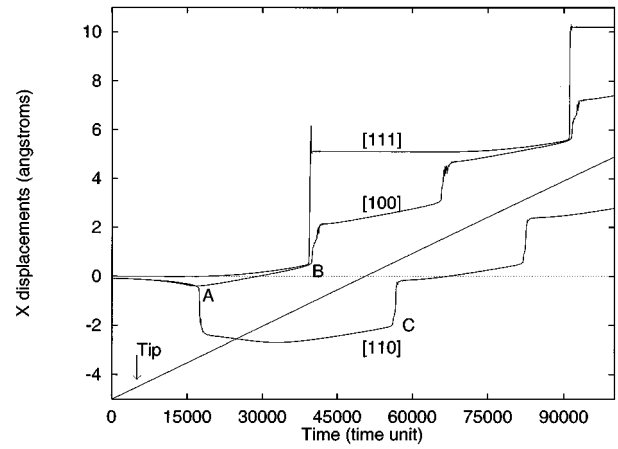

FIG. 7. Time-dependent motion of the xenon atom generated by a probe tip along a Cu(110) surface row (x axis). The minimal tip-surface distance to succeed in the atomic manipulation is $z_t = 6.05$ Å, $z_t = 5.75$ Å, and $z_t = 5.90$ Å for, respectively, the [110], [100], and [111] oriented tips. The dragging process is different according to the tip structure: in one case ([110]), the Xe atom is pulled by the probe, while in the two other cases, the adsorbate is pushed by the tip. The letters A, B, and C refer to particular points of the motion (see the text).

energetic contributions coming from the edges of the tip apex are important and can induce a localized displacement of the adsorbate.

Position 4. The tip continues to push the xenon atom laterally, but the interaction becomes repulsive due to a diminution of the adsorbate-surface distance. At this point the tip position is $x_t = 0$ Å. When $x_t > 0$ Å, the process is reversible and the adsorbate is released (the global interaction is less repulsive) by the tip.

Position 5. Once more, the xenon reaches the position 3 ($x_t = 1.32$ Å) and is attracted by the tip up to $x = 0.41$ Å. The tip apex does not deform the potential surface enough to allow the adsorbate to follow the tip displacement. After this point, the tip is too far and the xenon atom finds an equilibrium position on the hollow site of the Cu(110) surface (position 1).

With the three kinds of tip apex structures considered here, we have determined the optimal tip-sample distance to successfully manipulate the xenon atom by varying the tip-sample distance with a vertical step $\Delta z_t = 0.05$ Å. Figure 7 represents the x positions of the Xe atom during the tip motion. For the [111] apex structure, the optimal height is $z_t = 5.90$ Å. The moving process is a pushing mode. In this case, the tip displaces the xenon atom along an atomic surface row (Fig. 5) from the central hollow site ($x = 0$ Å) to point B ($x \sim 0.5$ Å). The atom passes over the barrier and does not diffuse in the first hollow surface site located at 2.55 Å but to the next one at 5.1 Å. This effect is due to the low atomic density on the edges of this trigonal apex, which does not supply enough attraction on the xenon atom to retain it. When the tip surface is slightly decreased (5.80 Å), the adsorbate moves regularly by jumping from a given stable site to another hollow site.

For the [100] apex structure, the moving process is also a pushing mode with the tip located at $z_t = 5.75$ Å. The adsorbate is attracted in a first time (point A) and then repelled to

point B, where it diffuses to the neighborhood of the next hollow site. In this case, the copper atoms on the facets of the apex hold the xenon atom, which contributes to a smooth pushing mode.

Finally, at $z_t = 6.05$ Å a pulling mode is predicted for the [110] tip structure. The tip attracts the adsorbate (point A) to the hollow site at -2.55 Å during its approach. The probe follows its straight trajectory and passes on the xenon atom without repelling it. After this transitory regime at point C, the adsorbate is pulled to the central hollow site and is manipulated by the tip.

According to this analysis, it is clear that the tip apex structure, and thus the atomic density on the tip apex facets, plays an important role in the atomic manipulation process. A pure sliding mode, occurring when during all the process $|x - x_t| = 0$, is not efficient for this system. Nevertheless, the smallest distance $|x - x_t|$ is ~ 0.5 Å for the [110] tip apex, which can be attributed to a mixing of sliding and pulling modes. One way to discriminate between these manipulation modes is the calculation of the tunnel current signature associated with each mode.

B. Signature of the manipulation mode in the tunneling current

During a manipulation sequence, the tunneling current intensity can be recorded to follow the behavior of the adsorbate in the STM junction.[35] Furthermore, under the tip apex constraint, the adsorbate equilibrium distance will change from site to site on the surface leading to a modulation of the tunneling current. Therefore, the recorded current displays a signature related to the exact position of the adsorbate that can provide precious information.

For each time-dependent position of the Xe atom [the solution of Eq. (9)], the tunneling current intensity in the junction can be calculated using the STM elastic scattering quantum chemistry (ESQC) technique.[36-38] In the present section, we will restrict our computerized simulations to the so-called constant altitude mode because it is less consuming in computation time than the constant current mode.

The electronic structure of the Cu(110)/Xe/tip apex junction implemented in our STM-ESQC code has already been detailed.[39] As it was done in Sec. IV A, the junction is described atom by atom including the Cu(110) surface and the structure of the tip apex. An extended Hückel Hamiltonian is constructed with a double-ζ basis set and the tunneling current intensity is calculated within the ESQC approximation from the generalized Landauer formula.[40,41] The elements of the multichannel scattering matrix are calculated from a nonunitary transformation of the spatial propagator describing the Bloch waves. These waves coming from the bulk of the tip body or of the substrate are then scattered on the STM junction. The matrix elements of this propagator are obtained from a Hamiltonian given by the extended Hückel molecular orbital method.[42]

At each position of the tip apex, the Xe atom is free to relax during 100 time units by solving Eq. (9) and finds its equilibrium position (Fig. 7). Then a new tunneling current intensity is calculated for each relaxed position supposing a low bias voltage. This procedure supplies the conductance
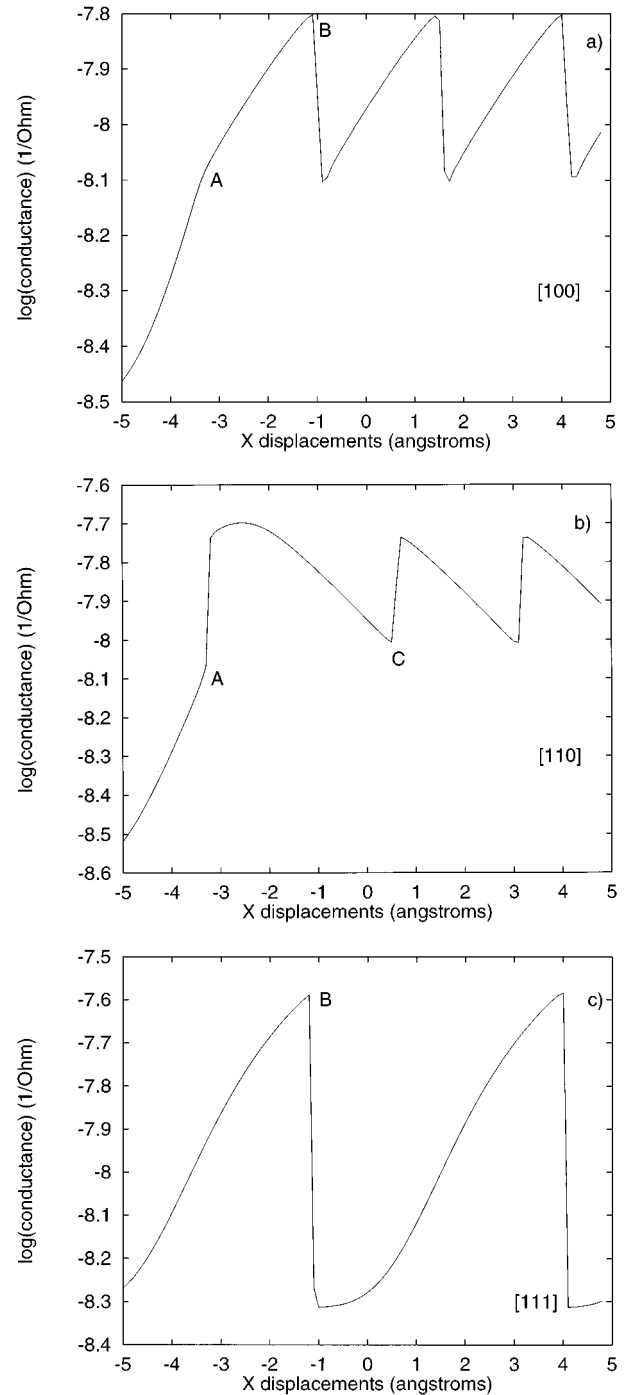

FIG. 8. Logarithm (base 10) of the tunneling conductance calculated during the moving process at constant tip-surface distance: (a) pushing process with a [100] oriented tip at 5.75 Å, (b) pulling process with a [110] oriented tip at 6.05 Å, and (c) pushing process with a [111] oriented tip at 5.90 Å. The letters A, B, and C refer to the same particular points as in Fig. 7.

variation of the junction during the entire manipulation sequence for the three tip structures considered here (cf. Fig. 8). For example, we can deduce from the conductance variation displayed in Fig. 8(a) that the adsorbate is continuously pushed by a tip of [100] geometry. In this case, to reach the Xe atom the tip apex needs to enter a quasirepulsive regime at the beginning of the manipulation sequence. Therefore,

the conductance increases from point A to point B. In a second step, due to the repulsive forces, the adsorbate escapes from the vdW trap and migrates towards the next hollow site. Consequently, in a short amount of time we observe a drastic decay of the conductance (point B). The tip then continues to move towards the new equilibrium position of the Xe atom leading to an increase of the conductance. It results in a sawtooth signal, which is characteristic of a pushing process.

Conversely, with a pulling process the tip apex begins by passing over the Xe atom, which constitutes the transitory regime described previously. As shown in Fig. 8(b), the Xe atom is attracted by the tip apex, which gives the abrupt conductance variation in point A. Afterward, at the moment when the tip apex passes over the atom, we observe a maximum in the conductance variation. Finally, the tip-adsorbate distance increases and the conductance decreases gently to reach point C. In this configuration, the tip apex is located beyond the adsorbate and attracts it in the next hollow site. A sawtooth signal is again observed, but now with an inversion of the appearance order of the conductance decays.

Another pushing process is characterized in Fig. 8(c) in the case of the [111] tip. When the Xe atom is repelled, it goes further away than in Fig. 8(a), which gives a large conductance decrease.

These calculations clearly demonstrate that to confirm the success of an atomic manipulation sequence, it is not necessary to wait for the STM image of the sample at the end of the process. Actually, a regular sawtooth signal is already a confirmation that the adsorbate is following the tip apex. Notice also that for the molecules manipulation process, the signals may be more complicated and can provide information on the molecular conformation changes during the repositioning.[43]

V. CONCLUSION

In this paper we have investigated the adsorption state of a xenon atom inside a complex STM junction. By using a discrete atomic representation of the copper tip apex and by solving a Dyson equation related to the dispersion equation of the system, we were able to calculate the N-body vdW energy of the Xe atom near the STM probe. Subsequently, we evaluated the vdW trap generated by the tip apex when the xenon atom is adsorbed on the Cu(110) surface.

A dynamical study has permitted us to revisit the manipulation process of a xenon atom by a metallic tip apex. According to the tip apex structure, the moving process is quite different: A pulling mode is found for the [110] tip and a pushing mode for both [100] and [111] tip geometries. The Cu(110)/Xe/tip apex junction has never reaveled a pure sliding mode, for which the adsorbate, placed just under the tip apex, follows the motion of the STM probe.

The discrimination between moving processes can be achieved by simultaneous recordings of the tunneling current intensity during the repositioning. In the constant height mode, we have demonstrated that the tunneling current signal reveals a sawtooth behavior. The rapid decay in the conductance represents the successive escapes of the xenon atom from a hollow site to another one. For instance, the particular shape of this signal indicates what kind of manipulation mode we are dealing with.

ACKNOWLEDGMENTS

---

*Electronic address: xavier.bouju@univ-fcomte.fr

†Present address: IPCMS, 23 rue du Lœss, F-67037 Strasbourg Cedex, France.

[1] D. Langbein, *Theory of van der Waals Attraction*, Springer Tracts in Modern Physics Vol. 72 (Springer-Verlag, Berlin, 1974).

[2] J. Mahanty and B. W. Ninham, *Dispersion Forces* (Academic, London, 1976).

[3] H. Margenau and N. R. Kestner, *Theory of Interatomic Forces*, 2nd ed. (Pergamon, Oxford, 1969).

[4] Y. Andersson, D. C. Langreth, and B. I. Lundqvist, Phys. Rev. Lett. **76**, 102 (1996).

[5] E. Hult, Y. Andersson, B. E. Lundqvist, and D. C. Langreth, Phys. Rev. Lett. **77**, 2029 (1996).

[6] Ph. Avouris, Acc. Chem. Res. **28**, 95 (1995).

[7] D. M. Eigler and E. K. Schweizer, Nature **344**, 524 (1990).

[8] M. F. Crommie, C. P. Lutz, and D. M. Eigler, Science **262**, 218 (1993).

[9] E. J. Heller, M. F. Crommie, C. P. Lutz, and D. M. Eigler, Nature **369**, 464 (1994).

[10] P. Zeppenfeld, C. P. Lutz, and D. M. Eigler, Ultramicroscopy **42-44**, 128 (1992).

[11] G. Meyer, S. Zöphel, and K.-H. Rieder, Phys. Rev. Lett. **77**, 2113 (1996).

[12] T. A. Jung *et al.*, Science **271**, 181 (1996).

[13] P. H. Beton, A. W. Dunn, and P. Moriarty, Surf. Sci. **361/362**, 878 (1996).

[14] M. T. Cuberes, R. R. Schlittler, and J. K. Gimzewski, Appl. Phys. Lett. **69**, 3016 (1996).

[15] M. T. Cuberes, R. R. Schlittler, and J. K. Gimzewski, Surf. Sci. **371**, L231 (1997).

[16] Ch. Girard, X. Bouju, and C. Joachim, Chem. Phys. **168**, 203 (1992).

[17] X. Bouju, C. Joachim, Ch. Girard, and P. Sautet, Phys. Rev. B **47**, 7454 (1993).

[18] J. R. Cerdá, P. L. de Andres, F. Flores, and R. Perez, Phys. Rev. B **45**, 8721 (1992).

[19] X. Bouju, C. Joachim, and Ch. Girard, Phys. Rev. B **50**, 7893 (1994).

[20] C. Joachim, X. Bouju, and Ch. Girard, in *Nanosources and Manipulation of Atoms under High Fields and Temperatures: Application*, Vol. 235 of *NATO Advanced Study Institute, Series E: Applied Science*, edited by Vu Thien Binh, N. García, and K. Dransfeld (Kluwer Academic, Dordrecht, 1993), pp. 239–252.

[21] X. Bouju, Ph.D. thesis, Université de Franche-Comté, 1993.

[22] A. Buldum, S. Ciraci, and Ş. Erkoç, J. Phys. Condens. Matter **7**, 8487 (1996).

[23] A. Buldum and S. Ciraci, Phys. Rev. B **54**, 2175 (1996).

[24] G. Vidali and M. W. Cole, Surf. Sci. **110**, 10 (1981).

[25] Ch. Girard and J. Humbert, Chem. Phys. **97**, 87 (1985).

[26] A. Glachant and U. Bardi, Surf. Sci. **87**, 187 (1979).
[27] E. G. Derouane, J.-M. André, and A. A. Lucas, J. Catal. **110**, 58 (1988).
[28] Ph. Lambin *et al.*, J. Chem. Phys. **90**, 3814 (1989).
[29] I. Derycke *et al.*, J. Chem. Phys. **94**, 4620 (1991).
[30] Ch. Girard and X. Bouju, J. Chem. Phys. **95**, 2056 (1991).
[31] O. J. F. Martin, Ch. Girard, and A. Dereux, Phys. Rev. Lett. **74**, 526 (1995).
[32] Ch. Girard and A. Dereux, Rep. Prog. Phys. **59**, 657 (1996).
[33] A. Yazdani, D. M. Eigler, and N. D. Lang, Science **272**, 1921 (1996).
[34] B. N. J. Persson, Surf. Sci. **269/270**, 103 (1992).

[35] G. Meyer and K.-H. Rieder (private communication).
[36] P. Sautet and C. Joachim, Chem. Phys. Lett. **153**, 511 (1988).
[37] P. Sautet and C. Joachim, Chem. Phys. Lett. **165**, 99 (1989).
[38] P. Sautet and C. Joachim, Chem. Phys. Lett. **185**, 23 (1991).
[39] C. Joachim, P. Sautet, and P. Lagier, Europhys. Lett. **20**, 697 (1992).
[40] R. Landauer, Z. Phys. B **68**, 217 (1987).
[41] R. Landauer, J. Phys. C **1**, 8099 (1989).
[42] R. Hoffmann, J. Chem. Phys. **39**, 1397 (1963).
[43] H. Tang, M. T. Cuberes, C. Joachim, and J. K. Gimzewski, Surf. Sci. (to be published).